accounts for the split Soret. However, the O_2 complex differs from the CO complex in two ways. The filled orbitals which have sulfur character also have oxygen character. In addition, the lowest empty orbital is an $O\pi^*$ orbital, absent in the carboxy complex, followed by the two $e_g\pi^*$ orbitals. Excitations from a_{1u} and a_{2u} to $O\pi^*$ as well as to $e_g\pi^*$ play a role in both components of the Soret band. This additional mixing leads to many more allowed transitions in the Soret region, causing the broadening and blue shift to λ 420 nm which has made the oxy P450 complex less easy to characterize. Such behavior should occur for reduced P450 whenever it has a second axial ligand which can interact with the porphyrin and iron π systems and the sulfur ligand. Work is continuing to determine the effect of variation in ligand geometry on these spectra.

Acknowledgment. We thank Dr. David Dolphin for making this unpublished data on oxy P450 available to us. We also thank Dr. Peter Debrunner for many helpful discussions and Visiting Scientist Dr. Amiram Goldblum for his interest and help in preparation of this manuscript. We also are grateful to Dr. Michael Zerner for his continued guidance in the use of his INDO program. We gratefully acknowledge support for this work from NIH Grant No. GM 27943 and from a National Resource for Computations in Chemistry (NRCC) computation award.

References and Notes

(1) Hanson, L. K.; Eaton, W. A.; Sligar, S. G.; Gunsalus, I. C.; Gouterman, M.; Connell, C. R. *J. Am. Chem. Soc.* **1976**, *98*, 2572.
(2) Hanson, L. K.; Sligar, S. G.; Gunsalus, I. C. *Croat. Chem. Acta* **1977**, *49*, No. 2, 237–250.
(3) Ullrich, V.; Ruf, H. H.; Wende, P. *Croat. Chem. Acta* **1977**, *49*, No. 2, 213–222.
(4) Churg, A. K.; Makinen, M. W. *J. Chem. Phys.* **1978**, *68*, No. 4, 1913–1925.
(5) Peterson, J. A.; Ishimura, Y.; Griffin, B. W. *Arch. Biochem. Biophys.* **1972**, *149*, 197–208.
(6) D. Dolphin, private communication.
(7) Chang, A. K.; Dolphin, D. *J. Am. Chem. Soc.* **1976**, *98*, 1607.
(8) Collman, J. P.; Sorrell, T. N. *J. Am. Chem. Soc.* **1975**, *97*, 4133–4134.
(9) Chang, A. K.; Dolphin, D. *Proc. Natl. Acad. Sci. U.S.A.* **1976**, *73*, No. 10, 3338–3342.
(10) Stern, J. O.; Peisach, J. *J. Biol. Chem.* **1974**, *249*, No. 23, 7495–7498.
(11) Ridley, J.; Zerner, M. *Theor. Chim. Acta* **1973**, *32*, 111.
(12) Ridley, J.; Zerner, M. *Theor. Chim. Acta* **1976**, *42*, 273.
(13) Bacon, A. D.; Zerner, M. C. *Theor. Chim. Acta* **1979**, *53*, 21.
(14) Rohmer, M. M.; Loew, G. H., *Int. J. Quantum Chem.*, in press.
(15) Herman, Z. S.; Loew, G. H. *J. Am. Chem. Soc.* **1980**, *102*, 1815.
(16) Zerner, M.; Loew, G. H.; Kirchner, R. F.; Mueller-Westerhoff, U. T. *J. Am. Chem. Soc.* **1980**, *102*, 589.
(17) Tang, S. C.; Koch, S.; Papaefthymiou, G. C.; Foner, S.; Frankel, R. B.; Ibers, J. A.; Holm, R. H. *J. Am. Chem. Soc.* **1976**, *98*, 2414–2434.
(18) Collman, J. P.; Gagne, R. R.; Reed, C. A.; Robinson, W. T.; Rodley, G. A. *Proc. Natl. Acad. Sci. U.S.A.* **1974**, *71*, 1326.
(19) Gouterman, M. In "The Porphyrins", D. Dolphin, Ed.; Academic Press: New York, 1977, Vol. III, p 1.

Gilda H. Loew*
Life Sciences Division, SRI International
Menlo Park, California 94025

Marie-Madeleine Rohmer
Quantum Chemistry Laboratory, University Louis Pasteur
Strassbourg F67000, France
Received October 5, 1979

Electronic Spectrum of Model Cytochrome P450 Complex with Postulated Carbene Metabolite of Halothane

Sir:

The widely used anesthetic halothane (2-bromo-2-chloro-1,1,1-trifluoroethane) undergoes oxidative metabolism by the cytochrome P450s in the presence of molecular oxygen and 2 reducing equiv of NADPH. While it was once believed that intermediate metabolic products from this oxidative metabolism in the pathway to forming trifluoroacetic acid[1] were responsible for observed renal and hepatic toxicity in man, there is now convincing evidence[2-4] that products of anaerobic reductive metabolism also catalyzed by cytochrome P450s[2,3] are the toxic substances. It is particularly interesting that, under anaerobic conditions (O_2 <50 μM), reduced cytochrome P450 in liver microsomal suspension forms a complex with halothane which exhibits an unusual Soret band at 470 nm. Such a spectrum has also been found in complexes of halothane with a reconstituted spherical phospholipid system containing rat or human cytochrome P450, reductase and NADPH.[5] This spectrum has been attributed to a ferrous cytochrome P450 complex in which a trifluoromethyl carbene (CF_3CH), formed by two-electron reductive elimination of chloride and bromide from the halothane molecule,[6] binds directly to the iron as an axial ligand.

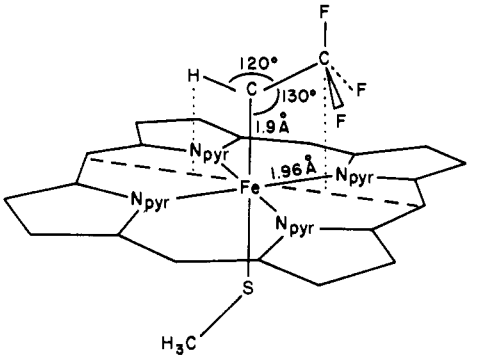

Figure 1. Model CF_3CH carbene P450 complex. Porphyrin and mercaptide ligand geometry was taken from model X-ray studies.[18] Carbene bond angles and torsion angles were chosen to minimize steric hinderance of CF_3 group with porphyrin ring with optimized C–Fe distance.

The most compelling evidence for the formation of such a carbene complex with ferrous cytochrome P450 is that an identical spectra is obtained in the presence of 2,2,2-trifluorodiazoethane. This species readily undergoes a metal-catalyzed decomposition to dinitrogen and the CF_3CH carbene.[6]

In both microsomal suspension[5,7,8] and reconstituted systems,[5] only difference spectra between the complex formed by addition of excess halothane and other complexes are obtained. For example, in the difference spectra between the carboxy and halothane complexes, the λ 450 nm band disappears and the λ 470 nm band appears. This is the only transition whose appearance is clearly demonstrated in observed spectra. It is not possible with membrane-bound cytochrome P450 to determine if there is another absorption band which corresponds to a second component of the Soret transition. In soluble carboxy $P450_{cAMP}$, this second band is found at ~363 nm, a region of intense protein absorption in both the reconstituted and microsomal systems of the carbene complex. Thus the question whether the postulated carbene complex, like the carboxy complex, has a split Soret spectrum is unresolved.

In the work reported here we have calculated the electronic spectrum of a model ferrous cytochrome P450–trifluoromethylcarbene complex, to further explore the hypothesis that a carbene complex of ferrous cytochrome P450 is responsible for the observed red-shifted Soret transition upon halothane addition, and to more fully characterize the spectrum of such a complex.

In this study, we have used a newly developed INDO method which includes transition metal complexes and extensive configuration interaction.[9-11] It has been used by us to successfully describe the ground-state and electronic spectra of oxy and carboxy P450,[12,13] oxy and carboxy heme complexes,[14-16] and ferrocene.[17]

The model carbene P450 complex used in this study is shown in Figure 1. The geometry of the porphyrin ring and methyl-

0002-7863/80/1502-3657$01.00/0

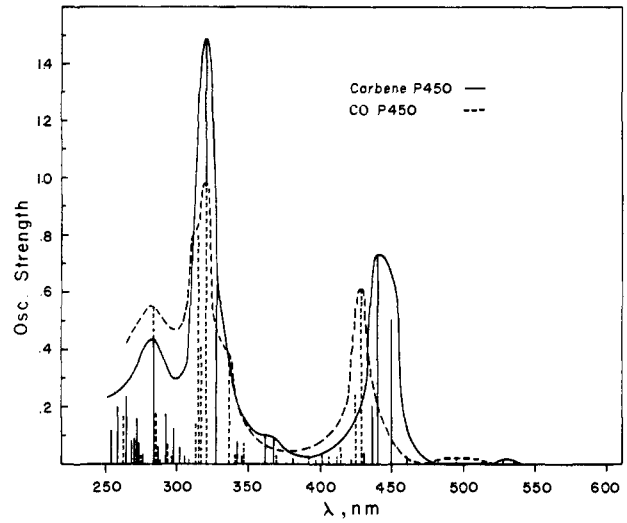

Figure 2. Calculated electronic transitions for model CF_3CH carbene P450 (—) and carboxy P450 (- - -) complexes.

mercaptide ligand is the same as in the previous study of the oxy and carboxy complexes. The carbene geometry used is shown in Figure 1. The Fe-C distance corresponds to an optimized value. Iron carbene angles were chosen to minimize steric hinderance of the CF_3 group with the porphyrin ring. Preliminary results with a totally optimized carbene complex indicate only a small effect on the calculated spectral transitions.

The calculated wavelength and oscillator strength of singlet-state electronic transitions for the P450 carbene complex is given in Figure 2 in the form of bar graphs. For comparison, the calculated spectra of the model carboxy P450 complex is also given. It is immediately apparent from this figure that the carbene complex has a red-shifted Soret transition relative to the carboxy complex in agreement with the observed behavior in difference spectra of halothane and carboxy complexes. It also appears that the carbene complex, in common with the carboxy complex, has a split Soret transition and the weaker visible absorption (Q_0) typical of all heme proteins.

In the calculation of these spectra, systematic configuration interaction was explored which included not only excitation from the a_{1u} and a_{2u} orbitals to the $e_g\pi^*$ orbitals, traditionally associated with the Q_0 and Soret transitions, but many other single and double excitations. The spectral transitions reported for the carbene are from a configuration interaction calculation including the most important 101 single and 70 double excitations and, for the carboxy, 63 single and 81 double excitations. Doubly excited configurations did not contribute >5% to any electronic transition in either complex. All allowed transitions had significant oscillator strength only in the heme (x,y) plane.

Table I gives the nature of the principal filled and virtual orbitals involved in the observed xy-allowed electronic transition of the carbene and carboxy complexes. While the molecular orbital scheme is very similar in the two complexes, both have explicit participation of the axial ligand in some of these MO's which accounts for observed differences between them. In both complexes, the splitting of the Soret bands is due to extensive mixing of $a_{1u},a_{2u} \rightarrow e_g\pi^*$ excitations with excitations from the four high energy sulfur-containing orbitals to $e_g\pi^*$. In addition, in the lower energy Soret band of the carbene spectrum which is red shifted from the carboxy band, there are significant contributions from $a_{1u},a_{2u} \rightarrow$ (carbene)* excitations. Transitions to CO* states are not significant in the carboxy complex. In the higher energy component of the Soret band in the carbene complex. there are major contributions from $d_{x^2-y^2} \rightarrow e_g\pi^*$, and all the sulfur-containing orbitals $\rightarrow d_{xy}^*$.

Three low-energy weak transitions are calculated at $\lambda \simeq 690$ nm, corresponding to Q_0 observed at 600 nm. However, only one of these is 100% $a_{1u},a_{2u} \rightarrow e_g\pi^*$, while others have ~25-50% $a_{1u},a_{2u} \rightarrow e_g\pi^*$ character, and 80% $d_{x^2-y^2} \rightarrow$ (carbene)* character.

The calculated spectrum obtained for the cytochrome P450-carbene complex strongly supports the suggestion that the observed spectra of halothane complexes with ferrous cytochrome P450 under anaerobic reductive conditions is indeed due to direct binding of a CF_3CH carbene product to the Fe of the protein. In agreement with the spectrum observed upon excess halothane addition to reduced cytochrome P450, the calculated spectrum shows a red-shifted Soret band relative to the carboxy complex. We also calculated an additional transition corresponding to a split Soret which is predicted to be under the intense protein transitions in the observed spectrum. To further verify the proposed origin of this spectrum, work is in progress on the possible role of other intermediates, particularly CF_3CCl, as both a ligand and a precursor to observed metabolic products.

Table I. Filled and Virtual Orbitals Involved in Allowed Electronic Transition of Model Ferrous Cytochrome P450

A. carbene (CF_3CH) complex		B. carboxy (CO) complex	
92	58% d_{xy}*	83	56% d_{xy}*
86	b_{2u}*	76, 77	85% CO*
85	65% carbene*; 30% d_{π}*	75	b_{2u}*
83, 84	$e_g\pi^*$; $e_g\pi^*$	73, 74	$e_g\pi^*$; 2% d_{π}*
82	99% a_{1u}	72	99 % a_{1u}
81	84% a_{2u}; 15% S_{π}; 1% carbene	71	84% a_{2u};15% S_{π}; 1% CO
80	33% d_{π}; 33% $S_{x,y}$; 15% carbene	70	65% $S_{x,y}$; 25% d_{π}; 3% CO
79	51% $S_{x,y}$; 23% d_{π}; 4% carbene	69	62% d_{π}; 2% S_{π}; 4% CO
78	50% d_{π}; 11% $S_{x,y}$	68	39% d_{π}; 25% S_{xy}; 2% CO
77	42% S_{π}; 10% d_{π}	67	50% S_{π}; 3% d_{π}
76	90% $d_{x^2-y^2}$	66	96% $d_{x^2-y^2}$

Acknowledgments. Support for this work from NIH Grant GM 27943 is gratefully acknowledged. A grant from the National Resource for Computation in Chemistry for computational costs is also acknowledged with thanks. Helpful discussions with Drs. M. M. Rohmer and M. C. Zerner are also appreciated. We are particularly thankful to Dr. James Trudell for suggesting this problem to us, guiding us to the appropriate literature, and discussing his unpublished work and its implications with us.

References and Notes

(1) Cohen, E. N. *Anesthesiology* **1969**, *31*, 560.
(2) van Dyke, R. A.; Wood, C. L. *Anesthesiology* **1973**, *38*, 328-332.
(3) van Dyke, R. A.; Wood, C. L. *Drug Metab. Dispos.* **1975**, *3*, 51-57.
(4) Uehleke, H.; Hellmer, K. H.; Tabarelli-Poplawski, S. *Naunyn-Schmiedberg's Arch. Parmakol.* **1973**, *279*, 39-52.
(5) James Trudell, Department of Anesthesiology. Stanford University Medical Center, private communication.
(6) Nastainczyk, N.; Ullrich, V.; Sies, H. *Biochem. Pharmacol.* **1978**, *27*, 387-390.
(7) Mansuy, D.; Nastainczyk, W.; Ullrich, V. *Arch. Pharmacol.* **1974**, *285*, 315-324.
(8) Uehleke, H.; Hellmer, K. H.; Tabarelli-Poplawski, S. *Arch. Pharmacol.* **1973**, *279*, 39-52.
(9) Ridley, J.; Zerner, M. C. *Theor. Chim. Acta* **1973**, *32*, 111.
(10) Ridley, J.; Zerner, M. C. *Theor. Chim. Acta* **1976**, *42*, 223.
(11) Bacon, A. D.; Zerner, M. C. *Theor. Chim. Acta* **1979**, *53*, 21.
(12) Rohmer, M. M.; Loew, G. H. *Int. J. Quantum Chem.*, in press.
(13) Loew, G. H.; Rohmer, M. M. *J. Am. Chem. Soc.*, preceding paper in this issue.
(14) Herman, Z. S.; Loew, G. H. *J. Am. Chem. Soc.* **1980**, *102*, 1815.
(15) Loew, G. H.; Herman, Z. S.; Zerner, M. C. *Int. J. Quantum Chem.*, in press.

(16) Herman, Z. S.; Loew, G. H.; Rohmer, M. M. *Int. J. Quantum Chem.*, submitted for publication.
(17) Zerner, M. C.; Loew, G. H.; Kirchner, R. F.; Mueller-Westerhoff, U. T. *J. Am. Chem. Soc.* **1980**, *102*, 589.
(18) Tang, S. C.; Koch, S.; Papaefthymiou, G. C.; Foner, S.; Frankel, R. B.; Ibers, J. A.; Holm, R. H. *J. Am. Chem. Soc.* **1976**, *98*, 2414-2434.

Gilda Loew*
Life Sciences Division, SRI International
Menlo Park, California 94025

Amiram Goldblum
Department of Pharmaceutical Chemistry
School of Pharmacy, Hebrew University of Jerusalem
Jerusalem, Israel

Received October 5, 1979

A Reversible Field Induced Phase Transition in Semiconducting Films of Silver and Copper TNAP Radical-Ion Salts

Sir:

The electron-accepting molecule 11,11,12,12-tetracyano-2,6-napthoquinodimethane (TNAP) has been shown to produce electrically conducting solids with aromatic heterocyclics and with alkali and divalent transition metal counterions.[1] In many cases, these charge-transfer complexes have exhibited higher conductivities than the analogous tetracyanoquinodimethane (TCNQ) salts. Several authors[1,2] have noted changes in electrical conductivity due to phase transitions in both TCNQ and TNAP complexes; however, these instabilities have all been induced by varying the temperature of the material.

We report here that we have observed a reversible electric field induced phase transition in polycrystalline aggregates of copper or silver TNAP radical-ion salts. This phase transition is accompanied by an abrupt increase in the electrical conductivity of the organic semiconductor when the applied field surpasses a threshold value. This highly conductive state remains intact as long as the field is present. When the applied field is removed, the system can either return to the high impedance state or, in cases where a voltage significantly higher than the threshold voltage is used to induce the highly conductive state, the material will remain in the low impedance state after the applied field has been removed.

The metal-TNAP films are synthesized by placing a piece of either Cu or Ag metal foil into a boiling solution of dry and degassed acetonitrile which has been saturated with neutral TNAP. Immediately upon dipping the foil into the saturated solution, a direct oxidation-reduction reaction occurs in which the corresponding metal salt of the radical-ion TNAP is formed as a polycrystalline film (eq 1). The reaction can be terminated

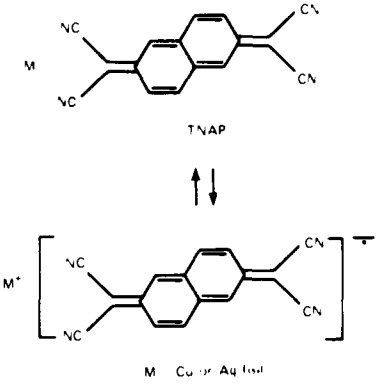

(1)

by simply removing the metal foil from the solution. Using this technique it is possible to grow a film that is in excess of five microns thick in less than one hour. Once the film has been grown to the desired thickness, it is removed from the solution and washed with additional acetonitrile to remove any neutral TNAP. The metal foil containing the charge-transfer salt is then dried under vacuum and an aluminum electrode[3] is evaporated on top of the polycrystalline film. Two electrical connections are then made to the laminated structure, one at the edge of the metal foil, and the other on top of the aluminum pad. Elemental analysis of the bulk of the polycrystalline film reveals that the metal-TNAP ratio is 1:1.[4]

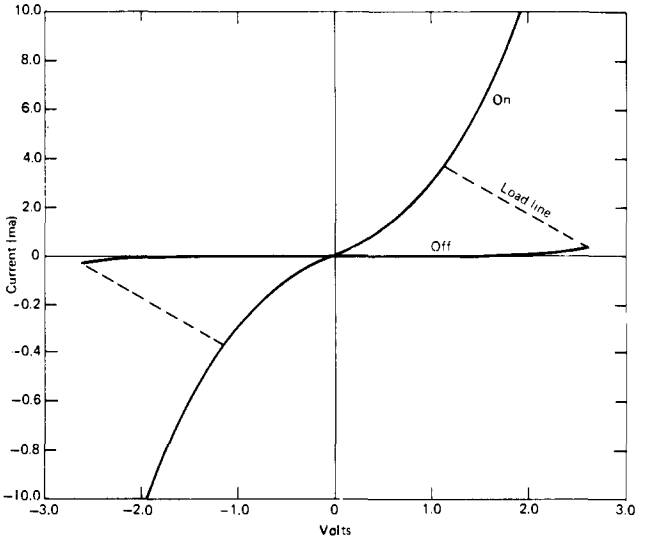

Figure 1. Current-voltage characteristic showing high- and low-impedance states for a 3.75μ Cu-TNAP sample.

Figure 1 shows a dc current voltage characteristic of a 3.75-μ-thick Cu-TNAP film made with a 100-Ω resistor as series load. Initially, at small applied voltages the impedance is $\sim 1.25 \times 10^4$ Ω. When the voltage across the sample surpasses a threshold voltage (V_{th}), the impedance of the sample rapidly drops to a value of 190 Ω. This switching from the high to low impedance state occurred at an applied potential of 2.7 V for this particular sample which corresponds to an applied field strength of $\sim 8.1 \times 10^3$ V/cm. Once the film has been placed in this highly conductive state, it will remain in this state as long as an applied voltage is present. Upon removing the applied voltage, the film will eventually return to its initial low conductivity state. The time required to switch back to the initial state appears to be directly proportional to the film thickness, duration of the applied voltage, and the amount of power dissipated in the sample while in the low impedance state. The electrical characteristics are only slightly dependent upon the direction of current flow and in a few cases a slight hysteresis is observed under conditions of high power dissipation.

Similar results are observed with Ag-TNAP films; however, these films do not exhibit the stability and reproducibility that is observed in the Cu-TNAP films. The impedance of a representative Ag-TNAP film is seen to drop abruptly from 2.4×10^5 to 2.8×10^3 Ω at a field strength of 6.0×10^3 V/cm. The film was ~ 7 μ thick.

Figure 2 is an oscilloscope trace of the voltage and current for a Cu-TNAP sample simultaneously displayed vs. time in response to an applied fast rise-time rectangular voltage pulse. The film originally in its high impedance state is switched to a low impedance state before the peak-applied voltage of the pulse generator was reached. Under these conditions, it is not possible to observe the conventional delay times and switching times as noted in inorganic materials;[5] however, from Figure 2 the combined delay and rise times appear to be less than a total of 4 ns (the limiting time of the pulse generator). In performing this experiment, a minimal overvoltage of 1.0 V was

0002-7863/80/1502-3659$01.00/0